Measuring U-Pb Zircon Ages in the Bear Island Granodiorite

By: Joseph Raum Advisor: Dr. Aaron Martin GEOL394 Spring 2008

# Table of Contents

Abstract	3
I. Introduction.	3
II. Geologic Setting A. Location and Extent	4
B. Geologic History and Age Constraints	4
III. Methods	5
IV. Data A. BIG-VA	6
B. BIG-MD	6
V. Calculation of Error.	7
VI. Interpretations and Discussions.	7
VII. Conclusions.	8
VIII. Acknowledgments	9
References	10
Figures	12
Tables	32
Appendix	36

#### **ABSTRACT**

In contrast to the adjacent Sykesville formation which has a large density of intrusive suites, the Mather Gorge formation within the Central Appalachian Potomac terrane has only a few igneous bodies. The Bear Island granodiorite outcrops at several locations within the  $50 \text{ km}^2$  migmatitic Bear Island domain, located in the regional Piedmont. Samples collected from two sites, one in Virginia and one in Maryland, were processed using mineral separation techniques in order to extract and ultimately date zircons by U-Pb methods. Laser ablation inductively coupled plasma mass spectrometry (LA-ICP-MS) analyses were performed at the University of Maryland. In order to obtain ages correlating to igneous crystallization, spot analyses were performed on grain margins along what were interpreted to be magmatic growth zones. Complications due to low ion counts by the mass spectrometer resulted in unusable data for the Maryland sample (BIG-MD). Large calculated ages (approximately 1200 Ma) for the Virginia sample (BIG-VA) reflect analysis of inherited material, which is common in the Piedmont zircons (Aleinikoff et al., 2002). However, a single grain produced an age of 571.1 Ma  $\pm$  37.4 (2 $\sigma$ ), corresponding to magmatic crystallization associated with early Appalachian orogenic events.

#### I. INTRODUCTION

Geochronology in the Central Appalachian Piedmont is limited due to poor exposures of bedrock, structural complexities, and the absence of fossils in many rock units (Muller et al., 1989). The recognition of cross-cutting igneous bodies within the terranes is therefore paramount to successfully unraveling the region's complicated history. Isotopic dating of igneous intrusions can provide lower age constraints for their host rocks as well as provide insights into timing of magmatic events. U-Pb dating of zircons in several Piedmont intrusive suites has provided geologists with not only lower constraints on depositional ages but also information pertaining to the early Appalachian orogenic events.

The Mather Gorge formation (figure 1), once described by Fisher (1970) and Drake (1989) as comprising a single prograde Barrovian metamorphic sequence of chlorite to sillimanite grade rocks, is now defined as a complex comprising at least two distinct tectonothermal domains (Kunk et al., 2005). The Bear Island granodiorite is one of few intrusive bodies identified. It is a fine-grained, leucocratic, muscovite-biotite granodiorite, occurring as sheets and cross-cutting bodies within the approximately 50 km<sup>2</sup> migmatitic Bear Island domain of the Central Appalachian Mather Gorge formation (figure 2) (Aleinikoff et al., 2002). Samples collected from both a Virginia and a Maryland outcrop (figures 1-5) were processed using mineral separation techniques in order to extract zircons and ultimately determine crystallization ages. Zircon extraction from the Virginia sample (BIG-VA) was performed at the University of Maryland using standard gravimetric and magnetic techniques. The Maryland sample (BIG-MD) was processed at Apatite to Zircon, Inc. in Viola, Idaho using similar techniques. The yields of the two samples were similar in both zircon abundance and morphology. Cathodoluminescence and photomicrograph images were taken for both samples at the University of Maryland in order to locate magmatic growth regions and inclusions. Isotopic dating using U-Pb methods was performed at the University of Maryland using laser ablation inductively coupled plasma mass spectrometry (LA-ICP-MS).

## II. GEOLOGIC SETTING

## A. Location and Extent

The Appalachian Mountains comprise five physiographic provinces, which from east to west are the Coastal Plain, Piedmont, Blue Ridge, Valley and Ridge, and Appalachian Plateau. The Piedmont extends from Alabama to Canada and is further divided in the Maryland and northern Virginia region into the Baltimore, Potomac, and Westminster terranes (figures 6 and 7) (Kunk et al., 2004). The study area is located in the Potomac terrane, within the central Appalachian Mountains. Here the Bear Island granodiorite outcrops in various locations in and around the migmatitic Bear Island domain.

The rocks of the Potomac terrane are described by Drake and Froelich (1997) as granofelsic metagraywackes, quartz-mica schists, and higher-grade equivalents. The terrane is constituted by three formations, each of which is separated by northeast trending faults. From east to west the formations are the Laurel, Sykesville, and Mather Gorge formations (figure 1) (Kunk et al., 2004). The Mather Gorge formation, bounded on the west by the Pleasant Grove fault and on the east by the Plummers Island fault, was divided by Kunk et al. (2004) into three domains based on differences in lithology, metamorphic history, structure, and geochronology. Furthest west is the Blockhouse Point domain, made of chlorite-sericite phyllonites and several ultramafic rock bodies. Next is the Bear Island domain, and it is described as garnet-sillimanite-grade metagraywackes and schists. The eastern portion is a migmatitic belt extending roughly 2 km east to west and 25 km north to south (Kunk et al., 2005). Additionally, large ultramafic rock bodies, granodiorites, pegmatites, amphibolites, and lamprophyre dikes are characteristic of the Bear Island domain. The easternmost domain is the Stubblefield Falls domain, including migmatitic schist that has retrograded to chlorite-sericite phyllonic schists. Also included in this domain are small amphibolite and granodiorite bodies.

# B. Geologic History and Age Constraints

The Appalachian Mountains are the product of a series of orogenic events between the Laurentian margin (present day eastern North America) and several volcanic island arcs and proto-continents. Prior to the first event, during the Late Proterozoic, rifting of Laurentia and Southern Rodinia resulted in the formation of the Iapetus Ocean. The Potomac terrane protoliths were deposited in this basin as distal slope deposits and olistrosomes. The Mather Gorge formation, in particular, was deposited as thick sequences of turbidites (Drake and Froelich, 1997). The rocks of the Mather Gorge formation are interpreted as having been part of a slab that was subducted under the Sykesville trench sediments (Kunk et al., 2005).

The first orogenic episode, the Penobscottian Orogeny, occurred between 520-490 Ma and resulted in the Potomac terrane's accretion to Laurentia (Kunk et al., 2005). Kunk et al. (2005) interprets amphibole and muscovite  $^{40}$ Ar/ $^{39}$ Ar ages of 455  $\pm$  23 Ma and 422 Ma (figures 8 and 9) to represent cooling of the Bear Island domain through 500°C and 365°C, respectively, corresponding to Penobscottian cooling.

Thrusting along the Pleasant Grove fault initiated during the Taconian Orogeny (470-440 Ma), causing movement of the Potomac terrane over the Westminster terrane (Kunk et al., 2004). Ordovician granitic intrusions corresponding to the timing of the Taconian collision are thought to be dominantly responsible for the regional metamorphism experienced by these Piedmont rocks. Among the oldest of these is the Georgetown Intrusive Suite, which intruded the Sykesville formation at approximately  $472 \pm 4$  Ma, based on  $^{206}\text{Pb}/^{238}\text{U}$  ages obtained from

sensitive high resolution ion microprobe analysis (SHRIMP) (Aleinikoff et al., 2002). The Occoquan granite, an intrusion in the Mather Gorge formation, was also emplaced at approximately  $472 \pm 4$  Ma, based on the methods just mentioned. Muth et al. (1979) dated muscovite from the Bear Island granodiorite using Rb/Sr techniques, and produced a cooling age of  $469 \pm 20$  Ma, which is interpreted to be the age of cooling through  $500^{\circ}$ C.

In contrast to the Taconian Orogeny, the Acadian Orogeny (400-380 Ma) was not a primary contributor to Central Appalachian metamorphism (Horton et al., 1989). The Bear Island domain's continuous cooling throughout the Ordovician and Late Carboniferous reflects the insignificant role or the Acadian event (figure 10) (Kunk et al., 2004). However, peak metamorphism in the adjacent Stubblefield Falls and Blockhouse Point domains was reached later, corresponding to Acadian activity. The Stubblefield Falls domain shared a similar history with the Bear Island domain but underwent Devonian metamorphism as the adjacent Sykesville formation began thrusting along the Plummers Island fault (Kunk et al., 2005). Stubblefield Falls  $^{40}$ Ar/ $^{39}$ Ar muscovite cooling age minima ranging from 375 to 350 Ma (figure 11) show a general age decrease towards the Plummers Island fault, where ages are similar to muscovite cooling ages of the Sykesville formation (Kunk et al., 2005). These cooling ages likely represent thermal resetting due to thrusting along the fault (Kunk et al., 2005). Similarly, the Blockhouse Point domain reached peak metamorphic conditions in the Middle Devonian, as supported by  $^{40}$ Ar/ $^{39}$ Ar muscovite cooling and growth ages of 371 Ma and 362 Ma, respectively (Kunk et al., 2005).

The contrasting ages across the Mather Gorge formation support the notion that the complex consists of at least two distinct tectonothermal domains and is not a single prograde Barrovian metamorphic sequence of chlorite to sillimanite grade rocks, as formerly described by Fisher (1970) and Drake (1989).

## III. METHODS

Rock samples were obtained from two Bear Island granodiorite outcrops using sledgehammers and a chisel. At each site, approximately three kilograms of granodiorite were collected. In addition, strike and dip measurements of joints, foliation and bedding were taken where possible (table 1). Instruments used include a Global Positioning System (GPS) and a Brunton compass set at declination 10.5°.

BIG-VA was processed at the University of Maryland in the mineral separation facilities. The sample was transported to a clean storage facility where it was re-bagged and shelved. The rock was pulverized into sand-sized grains and sieved through 2 mm and 0.25 mm mesh. Material was then panned, dried, and poured through a Frantz Magnetic Barrier four times using progressive current (0.5, 1.0, 1.5, 2.25 amperes). Density separation using methylene iodide was accomplished by using six 100 mL plastic beakers, each filled with approximately 70 mL methylene iodide and 15 mL non-magnetic BIG-VA grains. Zircons were then hand picked under a microscope using tweezers and placed on double-sided tape for mounting. Fifty grains were initially mounted, however, several were lost during polishing and one was determined to not be a zircon. Epoxy was poured into a one-inch diameter ring and set to cure for more than twenty-four hours. The mount was then polished using 2500 grade and 3000 grade sandpaper and cut using pliers and a hacksaw. As a final step in the mount preparation, the mount was cleaned in a sonic water bath and then photographed under a microscope (figure 12).

For the purpose of evaluating the mineral separation procedures performed at the University of Maryland, BIG-MD was processed in a different facility by different technicians. Comparing the two yields helped with evaluating the in-house methods. BIG-MD was

processed at in Viola, Idaho at Apatite to Zircon, Inc. The extracted zircons were returned in a 20 mL vial. Similar zircon quantity and morphology was recognized between the two samples. This reinforced the positive opinions regarding the University of Maryland separation practices. The same picking and mounting procedures used for BIG-VA were used for BIG-MD (figure 13).

Both samples were imaged at the University of Maryland on a JXA-8900 electron probe micro-analyzer. Cathodoluminescence and photomicrograph images were taken to locate magmatic growth zones and inclusions and to create a base map for laser spot analysis (figure 14-16).

Both samples were analyzed at the University of Maryland using a Thermo-Finnigan Element2 single collector double-focusing magnetic sector inductively coupled plasma mass spectrometer (ICP-MS). The procedures used are modified from those described by Chang et al. (2006) for U-Pb zircon dating. Zircons were ablated with a New Wave UP-213 laser ablation system, and the ablated material was carried to the plasma by helium and argon gas. The primary and secondary standards used were Harvard Standard 91500 and Temora2, respectively. In addition, the mass spectrometer was tuned prior to the analytical sessions using the glass standard NIST 612. The laser parameters used for the ablation of BIG-VA and BIG-MD zircons are summarized in table 2. Data reduction was completed using Microsoft Excel.

#### IV. DATA

## A. BIG-VA

Thirty-nine spot analyses were completed using thirty-one grains. For all but eight laser spots, a 30  $\mu$ m diameter aperture was used. The remaining eight spots were given a 40  $\mu$ m diameter aperture. Because the study focuses on the most recent igneous crystallization ages, spot analyses were performed—where possible—on what were assumed to be magmatic growth zones (figures 14 and 15). In addition, two spots were performed on eight grains in attempt to make age comparisons between zones. Single spots were done on the remaining twenty-three grains.

Discordance among  $^{206}\text{Pb}/^{235}\text{U}$ ,  $^{207}\text{Pb}/^{206}\text{Pb}$ , and  $^{206}\text{Pb}/^{238}\text{U}$  ages were found in seven analyses (figure 17). These data may have resulted from age discrepancies between multiple zones that were ablated simultaneously. In turn, these data were not factored into the calculated ages (figure 18). The youngest age, determined by  $^{206}\text{Pb}/^{238}\text{U}$ , is 571.1 Ma  $\pm$  37.4 (2 $\sigma$ ) (figure 19). The oldest age, determined by  $^{207}\text{Pb}/^{206}\text{Pb}$ , is 1557.8 Ma  $\pm$  77.1 (2 $\sigma$ ) (figure 20). The average ages, determined by  $^{206}\text{Pb}/^{238}\text{U}$  and  $^{207}\text{Pb}/^{206}\text{Pb}$ , are 1193.2 Ma  $\pm$  74.7 (2 $\sigma$ ) and 1264.3 Ma  $\pm$  86.9 (2 $\sigma$ ), respectively. A summary of the isotopic ratios and calculated ages for each of the spot analyses is given in tables 3 and 4.

#### B. BIG-MD

Due to complications arising from low ion counts, data from this analytical session is unusable. A 15  $\mu$ m diameter laser aperture was used during the majority of the session instead of a 30  $\mu$ m diameter aperture, which was used during the majority of the BIG-VA session. Low ion count rates produced by the smaller spot size enhanced the effect of the background noise and thus disallowed accurate background subtraction. In addition, the appropriate method file may not have been used for this analytical session. The result of using the wrong file, which is one intended for high U and Pb count rates, is that the mass spectrometer was operating on analog mode and not counting mode for most of the session. In turn, the secondary electron multiplier

(SEM) did not function as it needed to for the low U and Pb analyses. The low ion counts thus inhibit accurate background subtraction, rendering the data unusable.

## V. CALCULATION OF ERROR

Uncertainty in measurements arises from several sources including instrumental mass discrimination, elemental fractionation, and common lead contamination. All three sources of uncertainty were accounted for in final error propagation.

Instrumental mass discrimination is constant as a function of time with LA-ICP-MS analyses, and therefore can be corrected to high precision by comparison to a multi-isotopic element of similar mass (Horn et al., 1999). Prior to the analytical sessions, the mass spectrometer was tuned using the NIST 612 glass standard. Tuning enables mass discrimination between the Pb-Pb, Pb-U, and Pb-Th isotopes (Horn et al., 1999).

Elemental fractionation results from differences in volatility and is produced at the laser ablation site. In the cases of <sup>206</sup>Pb/<sup>238</sup>U and <sup>206</sup>Pb/<sup>235</sup>U, <sup>206</sup>Pb is transported from the laser site to the mass spectrometer with great efficiency than either of the heavier <sup>235</sup>U and <sup>238</sup>U isotopes. In addition, the degree of fractionation increases as the ratio of crater diameter to crater depth decreases, likely due to the increasing uranium condensation along the crater walls as transport out of the crater becomes increasingly difficult (Horn et al., 1999). Because the crater diameter to depth ratio decreases as a function of ablation time, zircon standards can be used for calibration. Fractionation factors were thus calculated and applied to the zircon data in order to correct for elemental fractionation.

Lead contamination results from exposure of the zircons to the surrounding environment. Lead is on the instrument, the sample mount, the lab technicians who handle the mount, and on the zircons. In theory, correction is as simple as monitoring the <sup>204</sup>Pb signals during analytical sessions, but the presence of <sup>204</sup>Hg in the argon gas masks the low intensity <sup>204</sup>Pb signals, thus hindering correction (Chang et al., 2006). In order to properly correct for common lead, the <sup>202</sup>Hg and <sup>204</sup>(Pb + Hg) masses were first measured, and the <sup>204</sup>Hg blank corrected value was calculated. Next, by comparison with the natural <sup>202</sup>Hg/<sup>204</sup>Hg the blank corrected <sup>204</sup>Hg value was calculated. Finally this value was subtracted from the <sup>204</sup>(Pb + Hg) in order to determine the <sup>204</sup>Pb value.

# VI. INTERPRETATIONS AND DISSCUSSIONS

A minimum age of 571.1 Ma  $\pm$  37.4 (2 $\sigma$ ) determined from  $^{206}\text{Pb}/^{238}\text{U}$  corresponds to Early Paleozoic magmatic activity. The grain (figure 19) is approximately 100  $\mu$ m in diameter and was analyzed using a 40  $\mu$ m diameter laser spot. Based on the cathodoluminescence image, the ablated material appears to have originated from growth zones and not from an inherited component. Furthermore, the size of the spot relative to the region of growth upholds the likelihood that the laser did not overlap onto an inherited component. Thus, the calculated age of 571.1 Ma  $\pm$  37.4 (2 $\sigma$ ) may be the age of zircon crystallization.

Unfortunately, this age minimum is an anomaly in the data, and the majority of concordant ages produced from the BIG-VA analysis do not correspond to Paleozoic magmatic crystallization. The mean BIG-VA zircon ages determined by LA-ICP-MS from  $^{206}\text{Pb}/^{238}\text{U}$  and  $^{207}\text{Pb}/^{206}\text{Pb}$  are 1193.2 Ma  $\pm$  74.7 (2 $\sigma$ ) and 1264.3 Ma  $\pm$  86.9 (2 $\sigma$ ), respectively, suggesting that the analyzed material was inherited and not Paleozoic magmatic overgrowths. Although magmatic growth zones may have existed in the zircon grains, it is likely that the widths in the polished cross-sections were significantly smaller than 30  $\mu m$ —the smallest spot diameter used.

The large size of the magmatic region in the youngest grain, approximately 50  $\mu$ m, is therefore not representative of this zircon population.

Inherited cores are common in Paleozoic zircons found in Central Appalachian Piedmont igneous rocks (Aleinikoff et al., 2002). Much of the terrane formed as magmatic arcs before amalgamating with Laurentia. Formation of these zircons involved magmatic crystallization around detrital seed crystals, which were supplied by the respective terranes (Aleinikoff et al., 2002). Thus, a possible implication is that the age of an inherited core for a given zircon corresponds to the maximum age of the rock that was intruded by the igneous body. In the case of the Mather Gorge formation, an age determined from an analyzed core may correspond to the maximum age of the protolith deposition. Unfortunately, the significance is minimal because of the old ages, approximately 1200 Ma. Zircons are robust and so are reworked throughout the crust while maintaining original chemistry. The implications are less captivating than those that can be made from magmatic crystallization ages.

## VII. CONCLUSIONS

Isotopic dating of zircons extracted from igneous rocks within the Central Appalachian Piedmont has yielded lower age constraints for the intruded host rocks and has allowed geologists to make inferences regarding the timing of certain tectonic and magmatic events. Aleinikoff et al. (2002) used both sensitive high resolution ion microprobe (SHRIMP) and thermal ionization mass spectrometry (TIMS) techniques to determine zircon crystallization ages for a variety of intrusive bodies, most of which are outcropped in the Sykesville formation just east of the Mather Gorge formation. The calculated ages are all Ordovician or younger, the oldest of which is  $472 \pm 4$  Ma (SHRIMP). The Occoquan granite, one of the few intrusive bodies found in the Mather Gorge formation, shares this  $472 \pm 4$  Ma (SHRIMP) crystallization age. However, the two terranes do not share a common lithology or metamorphic history. More precise definition of the minimum age constraints for the Mather Gorge formation may allow a more accurate and perhaps a more unique history to be drawn.

Based on SHRIMP and TIMS ages found by Aleinikoff et al. (2002), the hypothesized age of the Bear Island granodiorite was approximately 500 Ma, corresponding to early Appalachian orogenic episodes. The unsuccessful analysis of BIG-MD is unfortunate because the smaller laser spot size may have isolated the presumably small (less than 20  $\mu$ m) magmatic growth zones and thus enabled crystallization ages to be determined. Ironically, the smaller aperture likely deterred accurate background subtraction. Analysis of BIG-VA produced a mean age of 1200 Ma. These ages imply that inherited zircon cores were being ablated during analyses. The 30  $\mu$ m diameter laser spot was too large for all but one analysis. An anomaly in the data is the only age that is considered to be representative of an Early Paleozoic magmatic crystallization event. The laser spot size relative to the apparent magmatic growth size seen in the zircon's cathodoluminescence image (figure 19), supports the possibility that the calculated age of 571.1 Ma  $\pm$  37.4 (2 $\sigma$ ) determined from <sup>206</sup>Pb/<sup>238</sup>U is the age of zircon crystallization. Unfortunately, this zircon is only one of thirty-one grains that produced a reasonable age.

Although only one zircon grain produced an age corresponding to Early Paleozoic magmatic crystallization, the data remains scientifically significant. Analyses of inherited zircons yielded ages corresponding to the initial formation of the minerals. Zircons are robust and therefore have long lifetimes in the planet's crust. They can be reworked while preserving their chemistry. The old ages calculated in this study are not useful for interpreting magmatic timing,

but they do offer information regarding the source. Learning what we can is scientifically valuable.

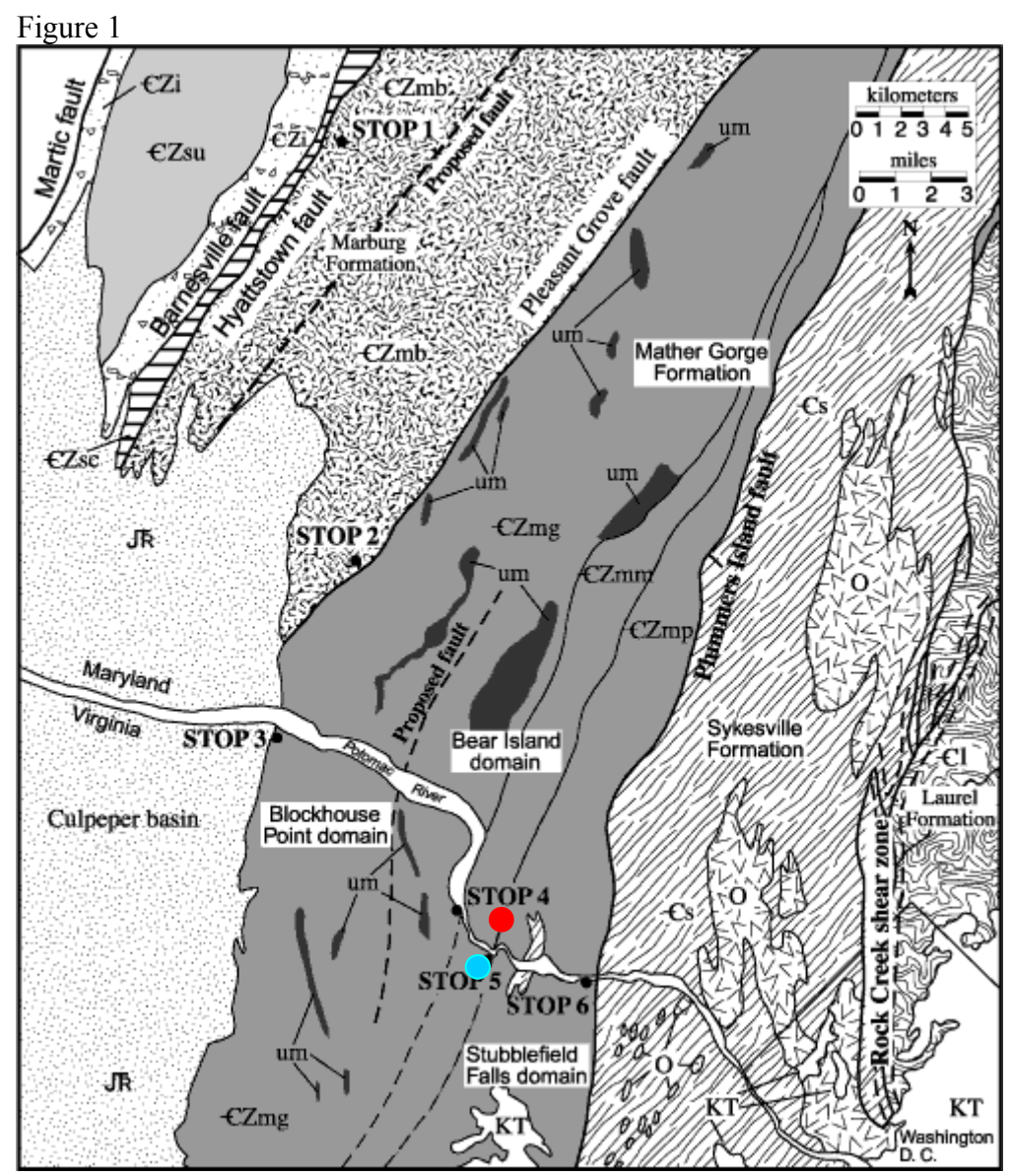
## VIII. ACKNOWLEDGEMENTS

I would like to thank several people for helping me complete this study and get through the year. Thank you to my advisor, Dr. Aaron Martin, for teaching me what I need to know to function as a geologist both in the field and in the lab. Also, for encouraging me to keep working whenever a problem would arise. Thank you to Dr. McDonough for being a crucial mentor during this second semester and teaching me that mineral extraction is only the beginning. In addition, thank you to Dr. Richard Ash and Dr. Saito (aka Tetsu) and all other technicians who assisted me with the laser analysis and data reduction. Thank you to all my professors in the department and my family and friends for supporting me. Finally, I would like to thank my fellow seniors and field camp companions for an unforgettable year.

## REFERENCES

- Aleinikoff, John, J. Horton, and Avery Ala Drake. "SHRIMP and Conventional U-Pb Ages of Ordovician Granites and Tonalites in the Central Appalachian Piedmont; Implications for Paleozoic Tectonic Events." <u>American Journal of Science</u> 302 (2002): 50-75.
- Carter, A, and C. S. Bristow. "Detrital Zircon Geochronology; Enhancing the Quality of Sedimentary Source Information Through Improved Methodology and Combined U-Pb and Fission-Track Techniques." <u>Basin Research</u> (2000): 47-57.
- Carter, B. T., J P. Hibbard, and M. Tubrett. "Detrital Zircon Geochronology of the Smith River Allochthon and Lynchburg Group, Southern Appalachians; Implications for Neoproterozoic-Early Cambrian Paleogeography." <u>Precambrian Research</u> 147 (2006): 279-304.
- Chang, Z., J. D. Vervoort, W. C. McClelland, and C. Knaack. "U-Pb Dating of Zircon by LA-ICP-MS." Geochemistry Geophysics Geosystems 7 (2006): 1-14.
- Drake, A. A., 1998, "Geologic map of the Kensington quadrangle, Montgomery County, Maryland": U.S. Geological Survey, scale 1:24,000.
- Drake, A.A., and A.J. Froelich., 1997, "Geologic map of the Falls Church Quadrangle, Fairfax and Arlington Counties and the City of Falls Church, Virginia, and Montgomery County, Maryland": US. Geological Survey, scale 1:24,000.
- Fisher, G.W. "The Metamorphosed Sedimentary Rocks along the Potomac River near Washington, D.C., *in* Fisher, G.W. et al., eds., Studies of Appalachian Geology, Central and Southern": New York, Interscience (1970), p. 299-315.
- Hatcher, R. D. "The Appalachians: an Accretionary and Collisional Orogen." Abstract. Geological Society of America 39 (2007): 36.
- Horn, I., R. L. Rudnick, and W. F. McDonough. "Precise Elemental and Isotope Ratio Determination by Simultaneous Solution Nebulization and Laser Ablation-ICP-MS: Application to U-Pb Geochronology." <u>Chemical Geology</u> 167 (1999): 405-425.
- Horton, J.W., A.A. Drake Jr., and D.W. Rankin. "Tectonostratigraphic Terranes and Their Paleozoic Boundaries in the Central and Southern Appalachians: Geological Society of America Special Paper 230 (1989), p.213-245.
- Krol, M. A., P. D. Muller, and B. D. Idleman. "Late Paleozoic Deformation Within the Pleasant Grove Shear Zone, Maryland; Results From (Super 40) Ar/ (Super 39) Ar Dating of White Mica." GSA Special Paper 330 (1999): 93-111.

- Kunk, M. J., R. P. Wintsch, C. W. Naeser, and N. D. Naeser. "Contrasting Tectonothermal Domains and Faulting in the Potomac Terrane, Virginia-Maryland; Discrimination by (Super 40) Ar/ (Super 39) Ar and Fission-Track Thermochronology." <u>Geological Society of America</u> 117 (2005): 1347-1366.
- Kunk, M. J., R. P. Wintsch, and S. C. Southworth. "Multiple Paleozoic Metamorphic Histories, Fabrics, and Faulting in the Westminster and Potomac Terranes, Central Appalachian Piedmont, Northern Virginia and Southern Maryland." <u>USGS Circular</u> (2004): 163-188.
- Kunk, M. J., R.P. Wintsch, S. C. Southworth, and B. K. Mulvey. "Constraints in the Thermal History of the Potomac and Westminster Terranes in Maryland, Virginia, and Washington D.C.; Extraction of Useful Ages From Complex (Super 40) Ar/ (Super 39) Ar Age Spectra." Abstract. Geological Society of America 36 (2004): 76.
- McDonough, W. F., 2008, personal communication.
- Muller, P. D., P. A. Candela, and A. G. Wylie. "Liberty Complex; Polygenetic Melange in the Central Maryland Piedmont." <u>GSA Special Paper</u> 228 (1989): 113-134.
- Muth, K., Arth, J. G., and J. C. Reed Jr., "A minimum age for high-grade metamorphism and granite intrusion in the Piedmont of the Potomac River Gorge near Washington, D. C." Geology 7 (1979): 349-350.
- Pyle, J. M., H. Bosbyshell, and G. Blackmer. "Refining the Metamorphic and Tectonic History of the Southeastern Pennsylvania Piedmont; Recent Results From Monazite and Zircon Geochronology and Accessory-Phase Thermometry." <u>GSA Field Guide</u> 8 (2006): 83-112.
- Southworth, S., A. A. Drake, and D. K. Brezinski. "Central Appalachian Piedmont and Blue Ridge Tectonic Transect, Potomac River Corridor." <u>GSA Field Trip Guide</u> 8 (2006): 135-167.
- Southworth, S., 1999, "Geologic map of the Urbana Quadrangle, Frederick and Montgomery Counties, Maryland: U.S. Geological Survey, scale 1: 24,000.
- Xia, X, M. Sun, and G. Zhao. "LA-ICP-MS U/Pb Geochronology of Detrital Zircons From the Jining Complex, North China Craton and Its Tectonic Significance." <a href="Precambrian Research">Precambrian Research</a> 144 (2006): 199-212.
- Yue, Y., S. A. Grahm, and B. D. Ritts. "Detrital Zircon Provenance Evidence for Large-Scale Extrusion Along the Altyn Tagh Fault." <u>Tectonophyics</u> 406 (2005): 165-178.



The formations of the Potomac terrane: from east to west, the Laurel, Sykesville, and Mather Gorge formations. The Mather Gorge formation is bounded on the east by the Plummers Island fault and on the west by the Pleasant Grove fault. €zmg—Mather Gorge formation, €mm—migmatitic Mather Gorge formation, €mp—chlorite-sericite phyllonite of the Mather Gorge formation, €mp—Marburg formation, €s—Sykesville formation, €l—Laurel formation, um—ultramafics. The outcrop locations for BIG-VA and BIG-MD are shown by the blue and red dots, respectively. (Kunk et al., 2004)



Virginia outcrop of the Bear Island granodiorite (light colored) seen in contact with migmatitic schist of the Mather Gorge formation (dark colored). Two cross-cutting dikes are seen trending diagonally across the picture. (Raum, 2007)



Virginia outcrop of the Bear Island granodiorite (light colored) seen in contact with migmatitic schist of the Mather Gorge formation (dark colored). (Raum, 2007)



Maryland outcrop of the Bear Island granodiorite. Large Pluton located near Old Anglers Inn. (Raum, 2008)

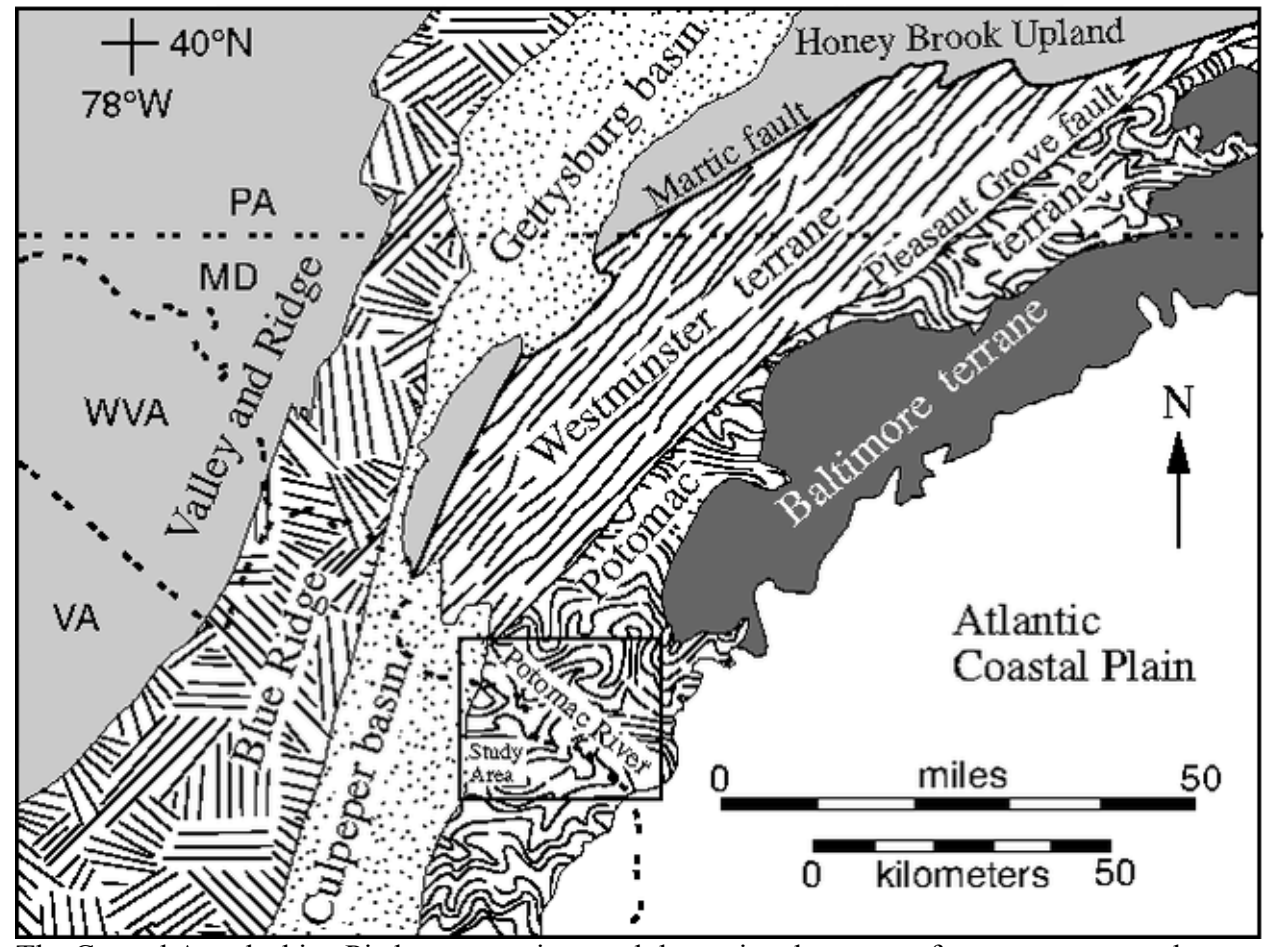


Maryland outcrop of the Bear Island granodiorite. Intrusion into metasedimentary rocks of the Mather Gorge formation located near Old Anglers Inn. (Martin, 2008)



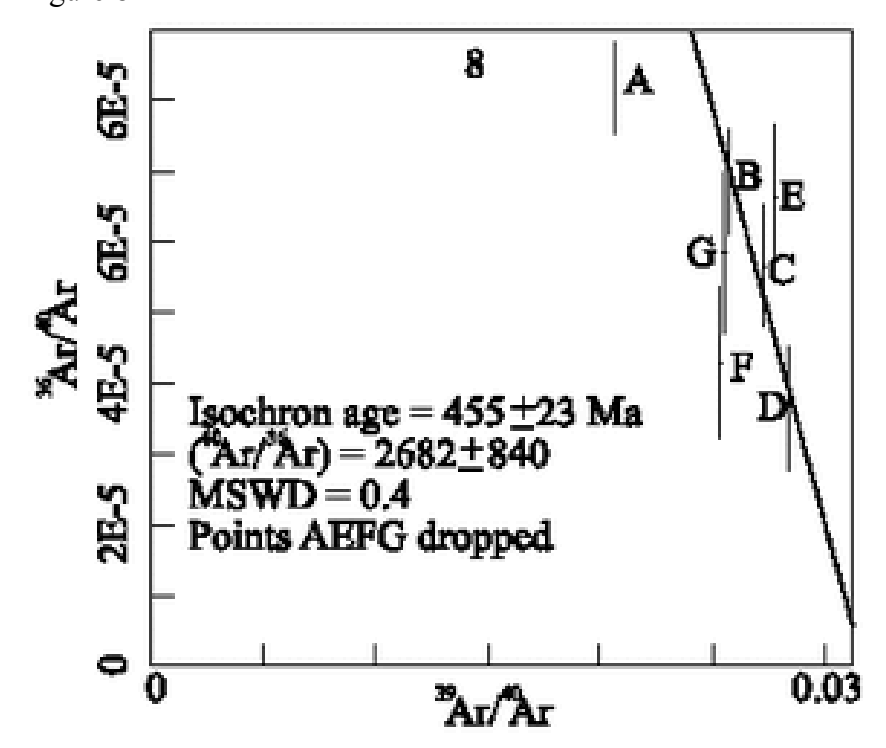
Physiographic map of the USA showing the approximate extent of the Appalachian Piedmont province. Modified (2007) from http://www.freeworldmaps.net/northamerica/index.html

Figure 7



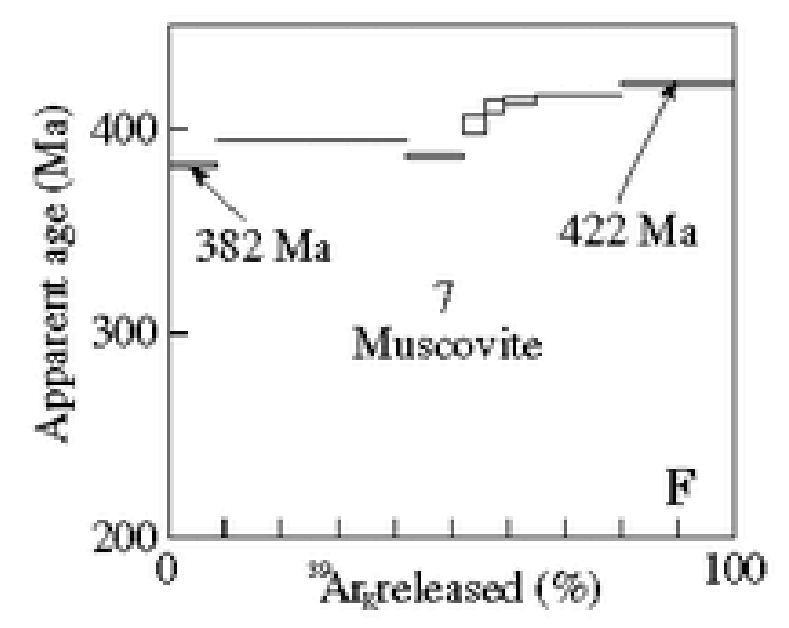
The Central Appalachian Piedmont province and the regional terranes: from east to west, the Baltimore, Potomac, and Westminster terranes. (Kunk et al., 2004)

Figure 8

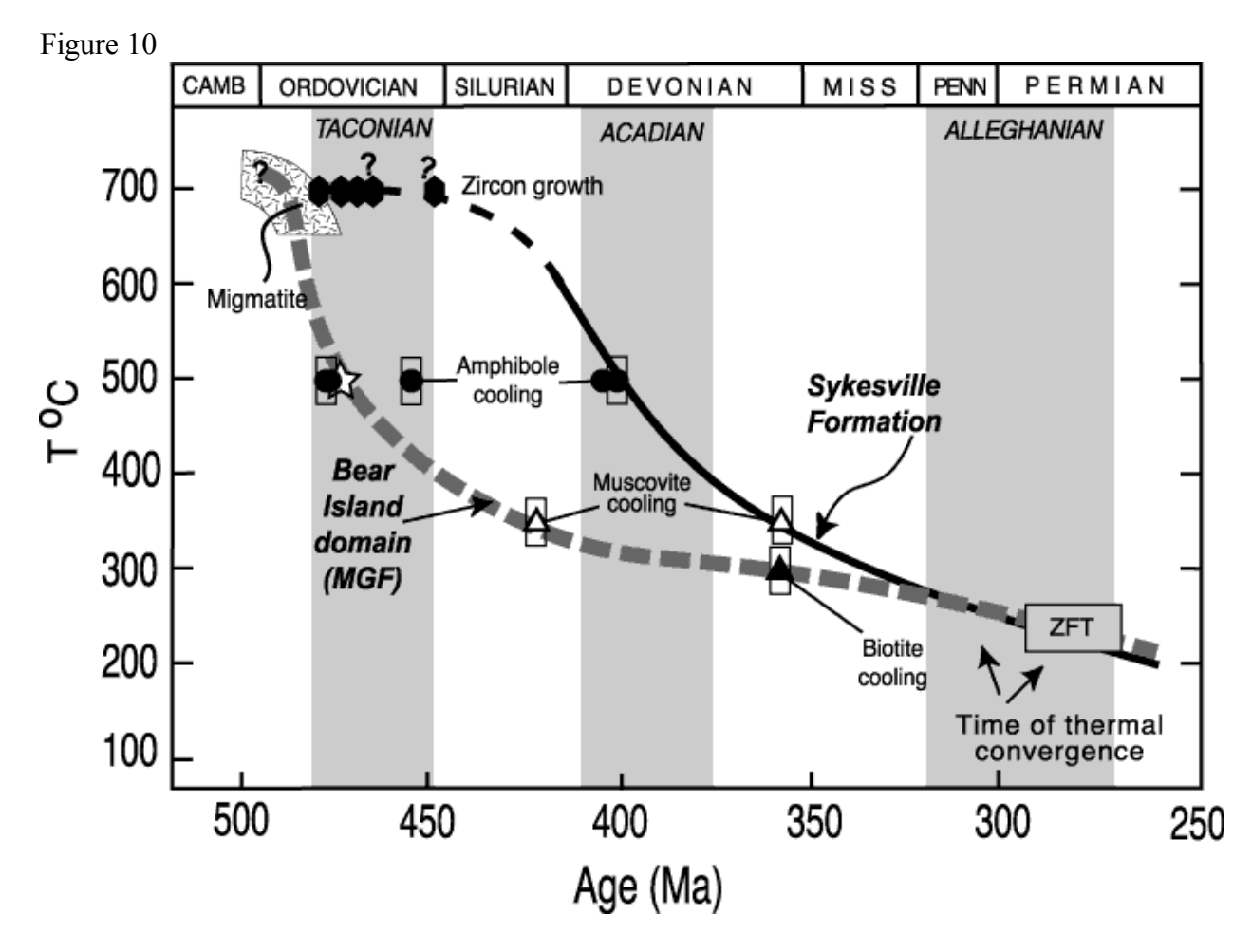


Inverse isochron diagram for Ar/Ar analysis of amphibole from the Bear Island domain.  $455 \pm 23$  Ma corresponds to the time at which the rock cooling through 500°C. (Kunk et al., 2005)

Figure 9

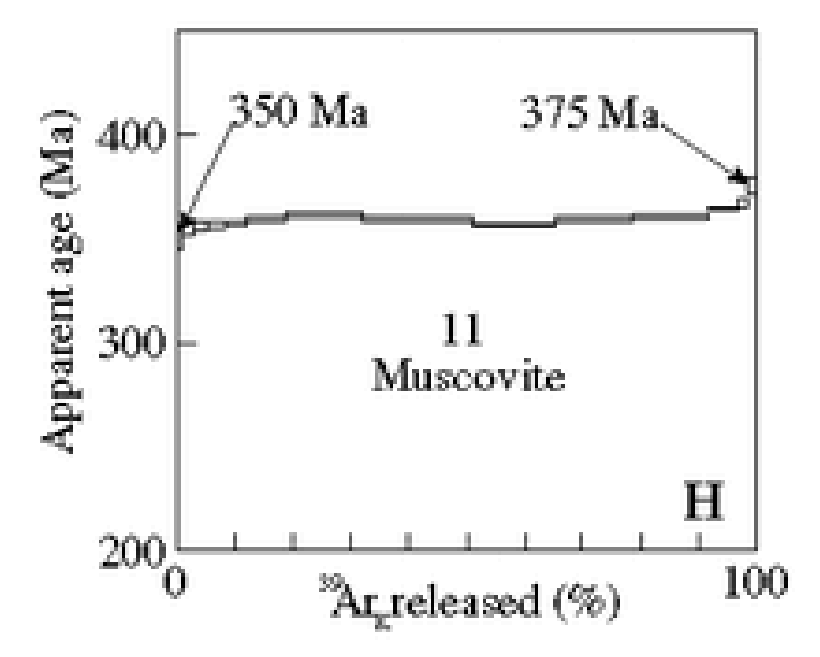


Age spectrum diagram for Ar/Ar analysis of muscovite from the Bear Island domain. 422 Ma corresponds to the time at which the rock cooled through 365°C. (Kunk et al., 2005)



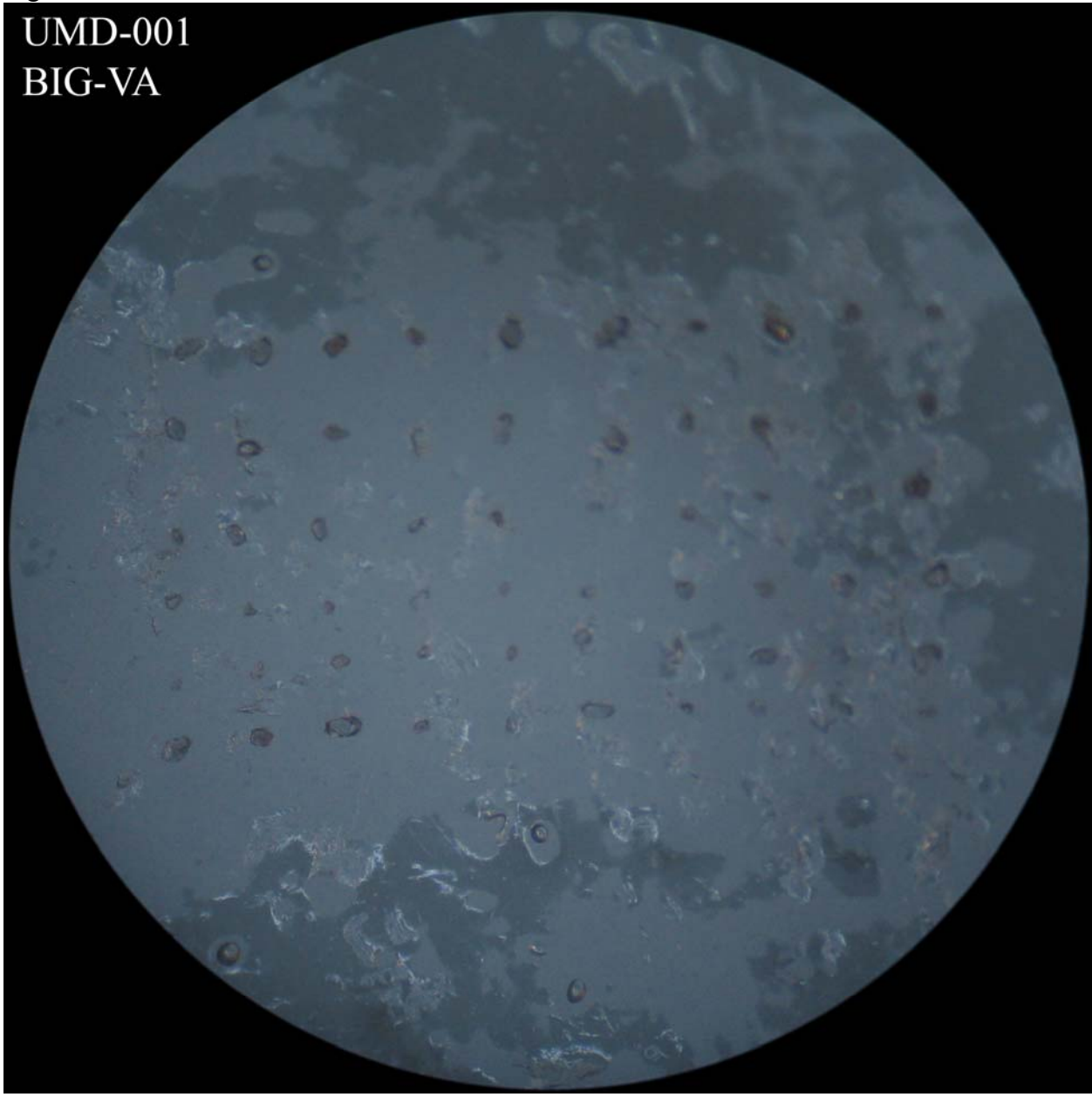
Cooling curves for the Bear Island domain of the Mather Gorge formation and the Sykesville formation. The Bear Island domain cooled continuously throughout the Ordovician to Carboniferous. (Kunk et al., 2004)

Figure 11



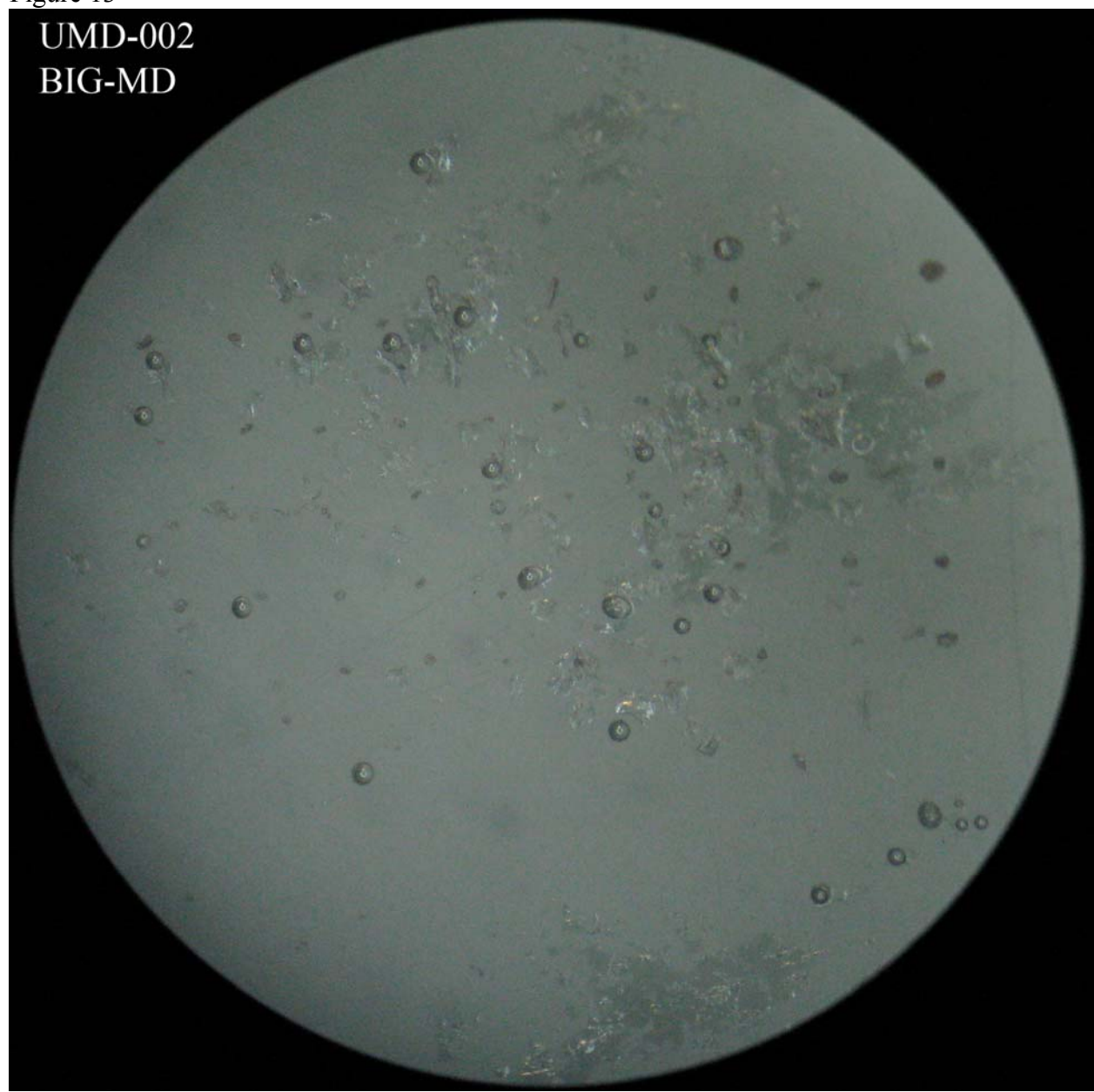
Age spectrum diagram for Ar/Ar analysis of muscovite from the Stubblefield Falls domain. 350 to 375 Ma corresponds to age minima range at which the rock cooled through 365°C. (Kunk et al., 2005)

Figure 12

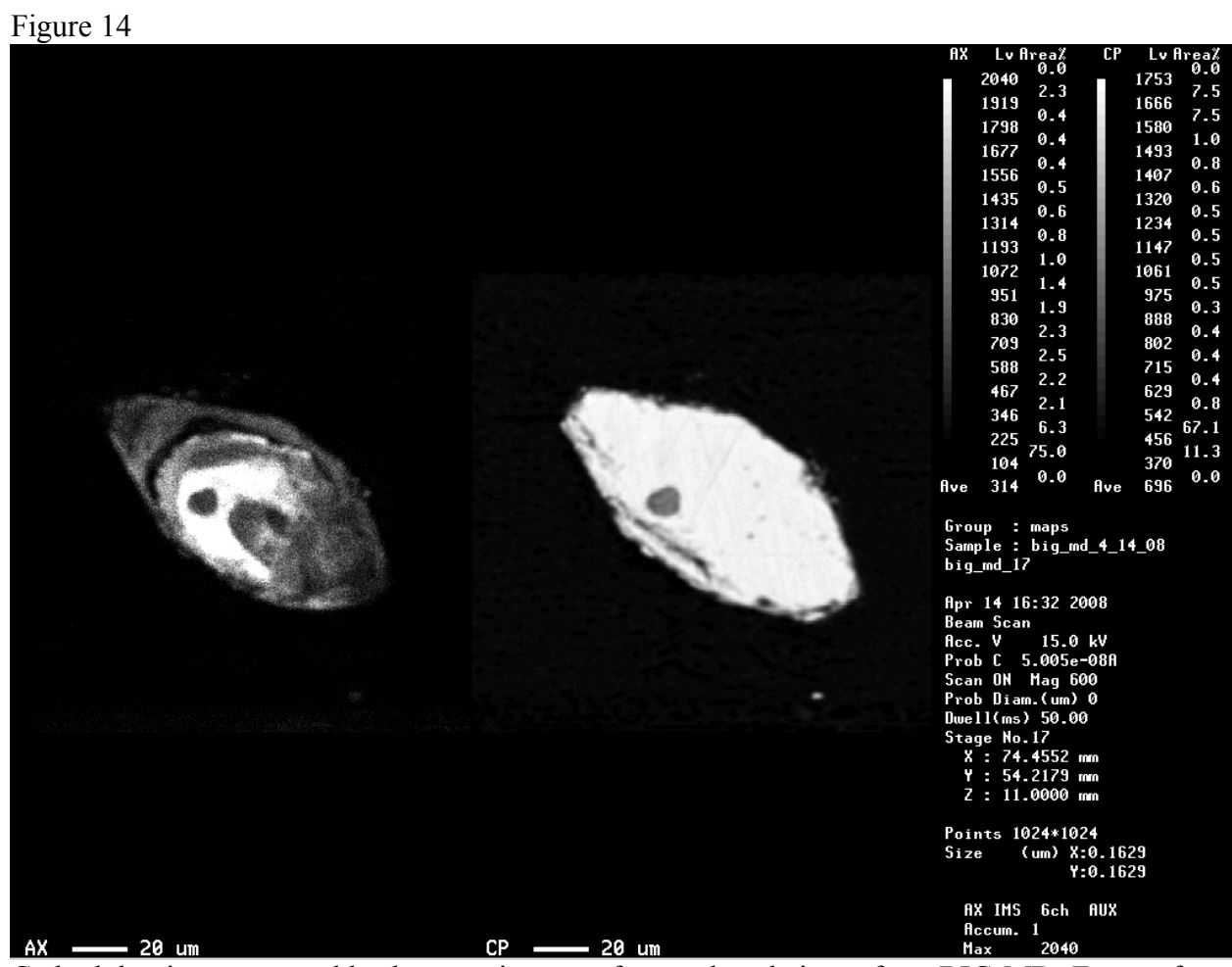


Photograph of unablated BIG-VA zircons taken under a microscope. (Raum, 2008)

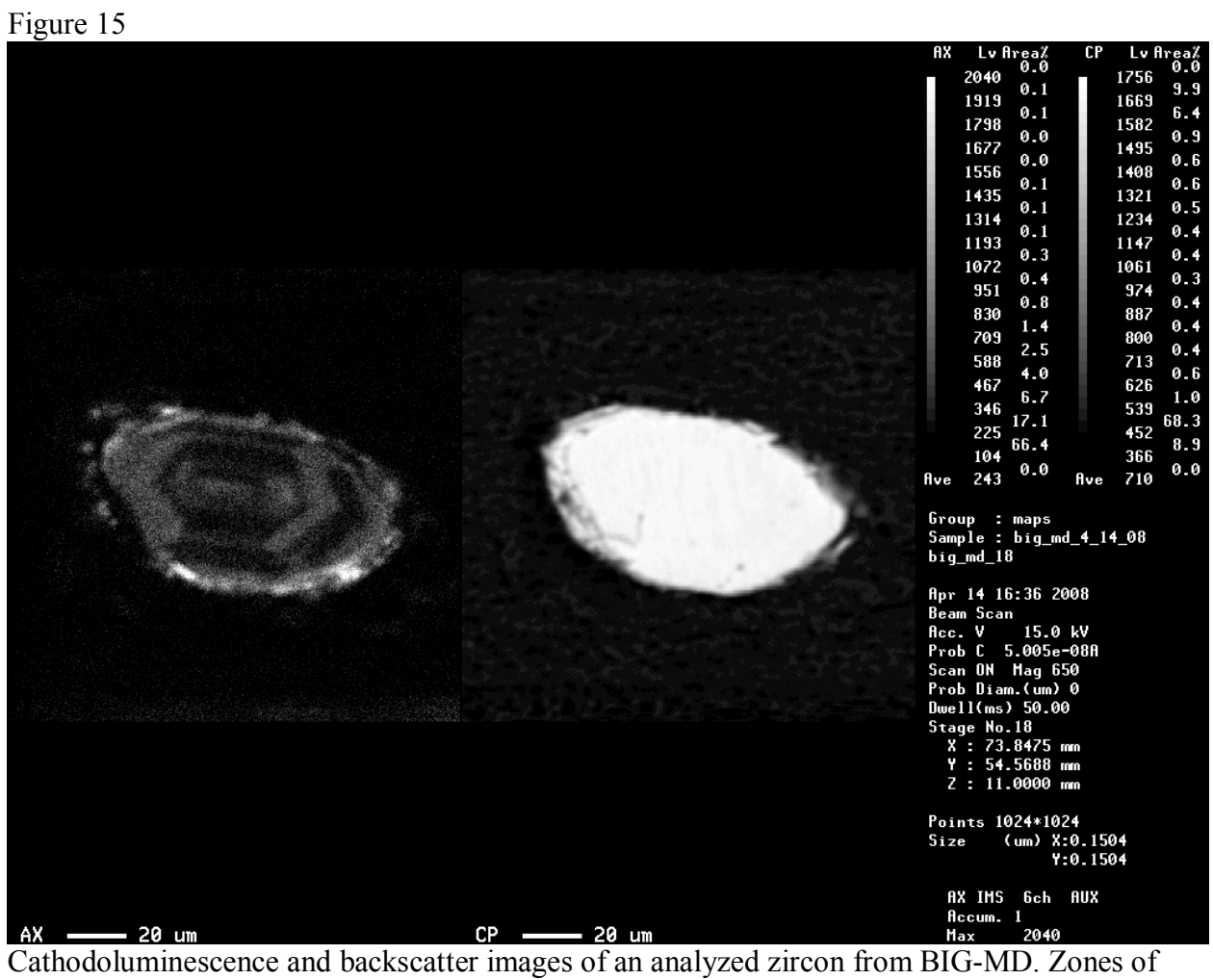
Figure 13



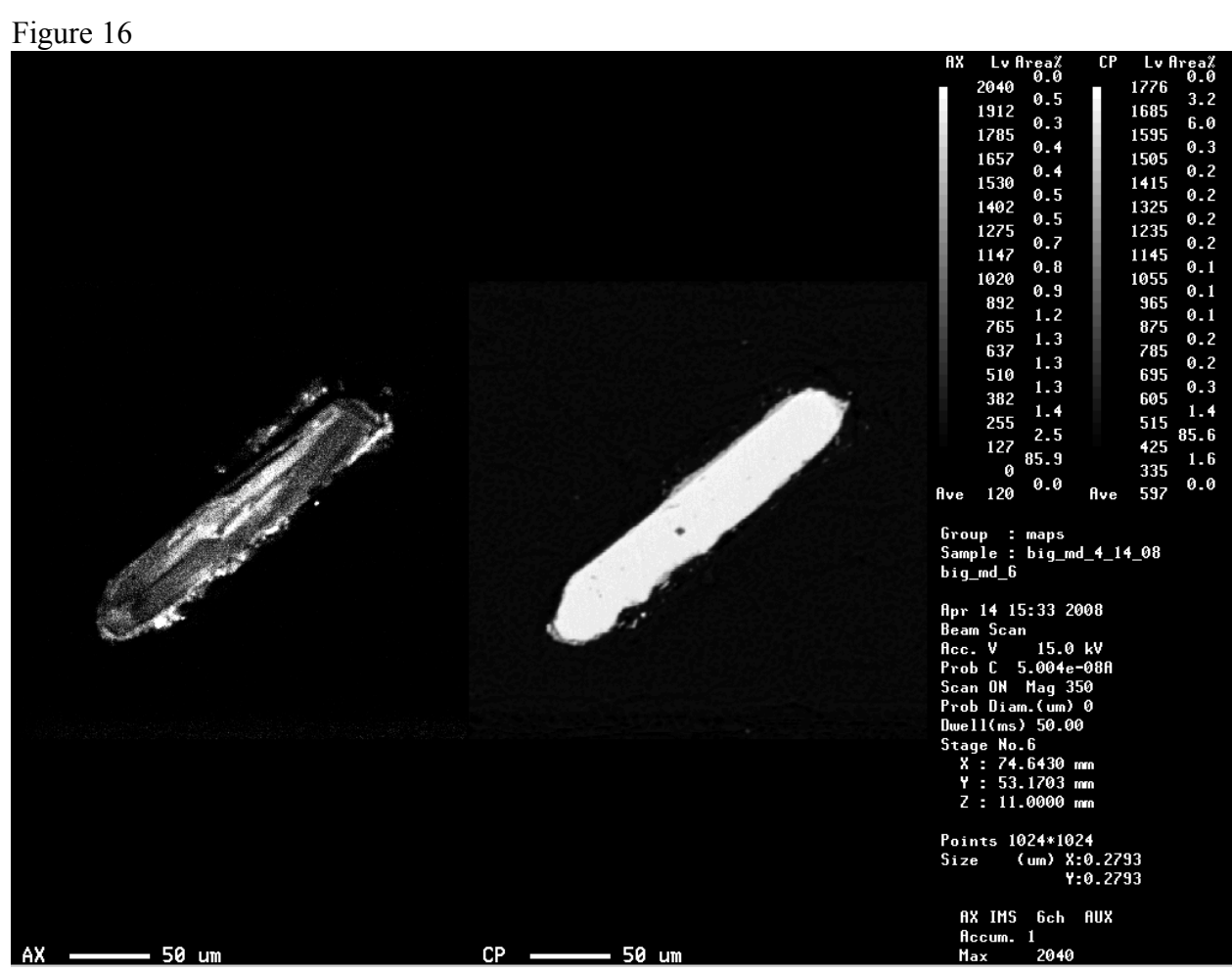
Photograph of unablated BIG-MD zircons taken under a microscope. (Raum, 2008)



Cathodoluminescence and backscatter images of an analyzed zircon from BIG-MD. Zones of growth are seen in the cathodoluminescence image (Raum, 2008)

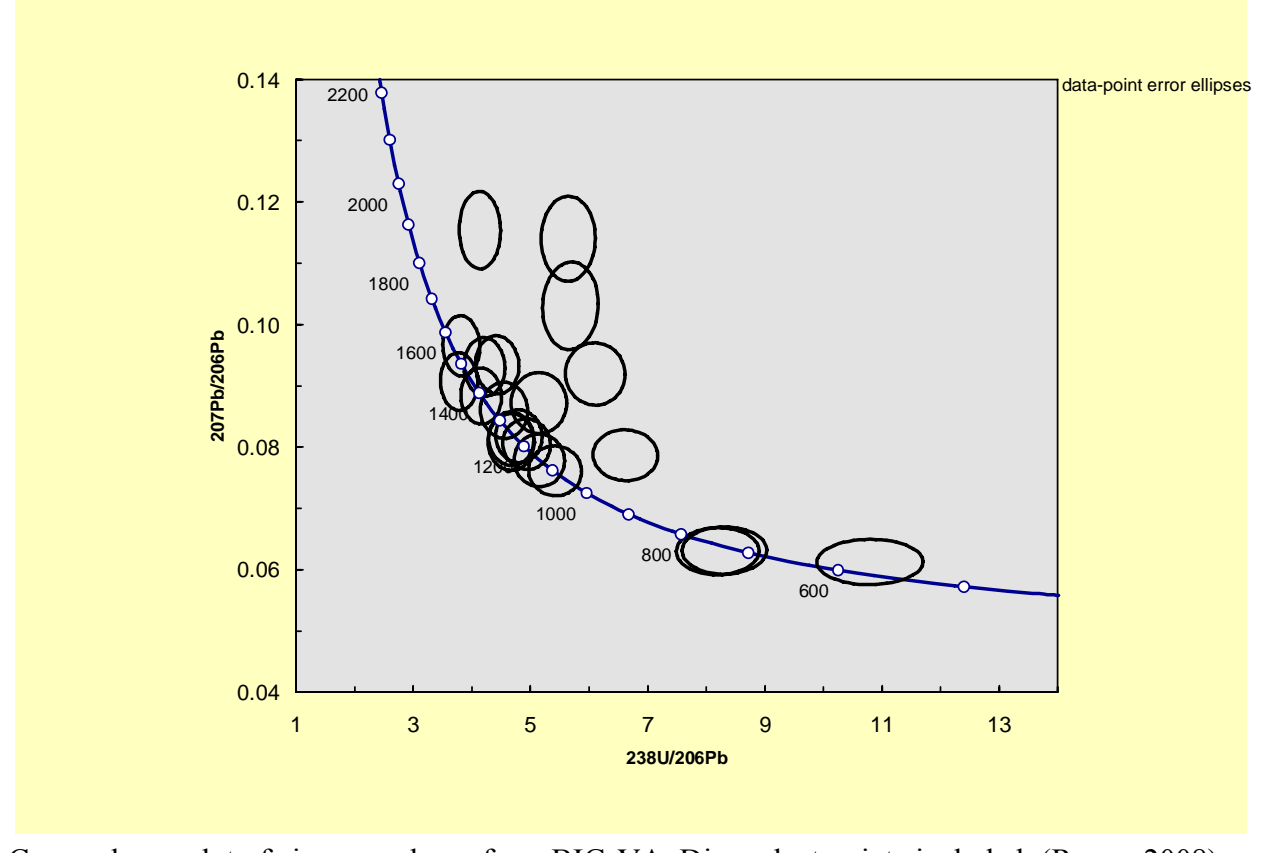


growth are seen in the cathodoluminescence image (Raum, 2008)



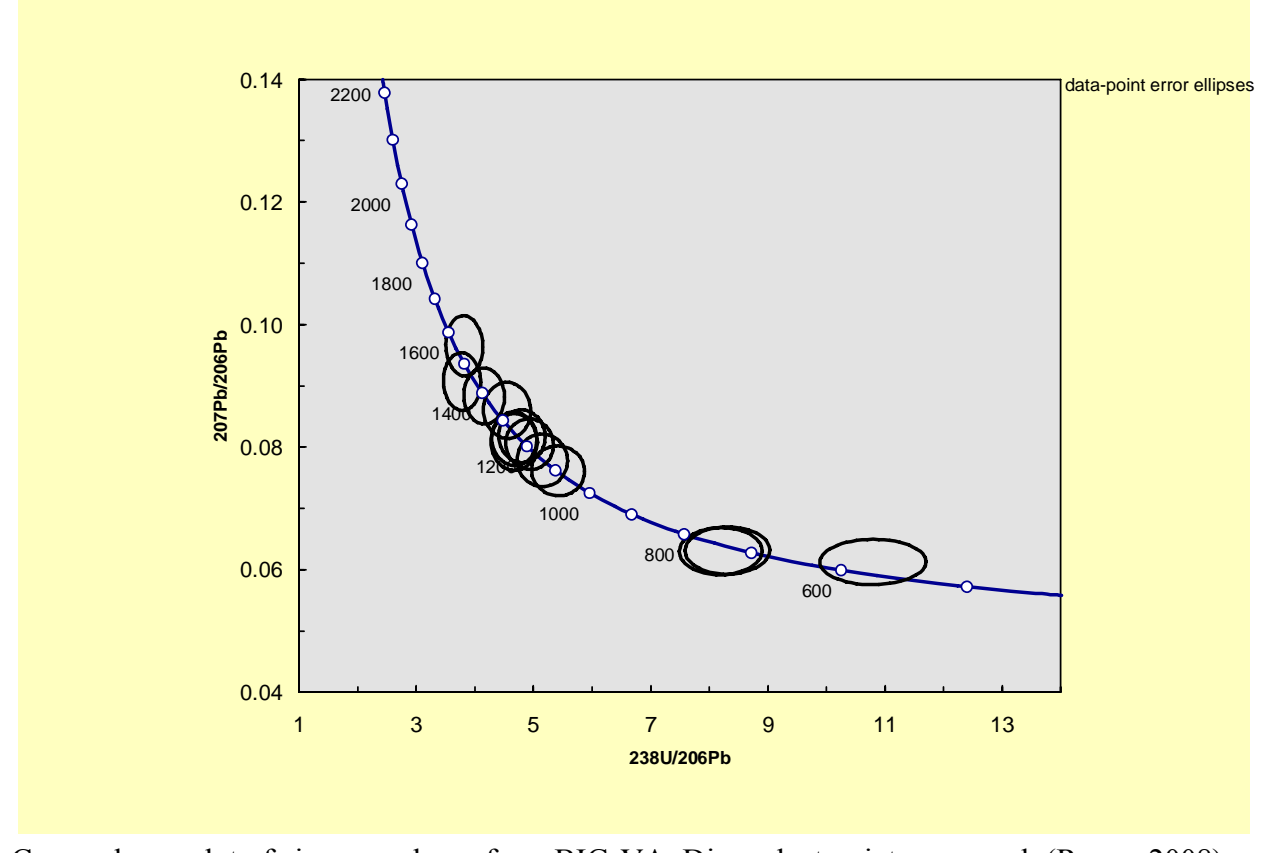
Cathodoluminescence and backscatter images of an analyzed zircon from BIG-MD. (Raum, 2008)

Figure 17



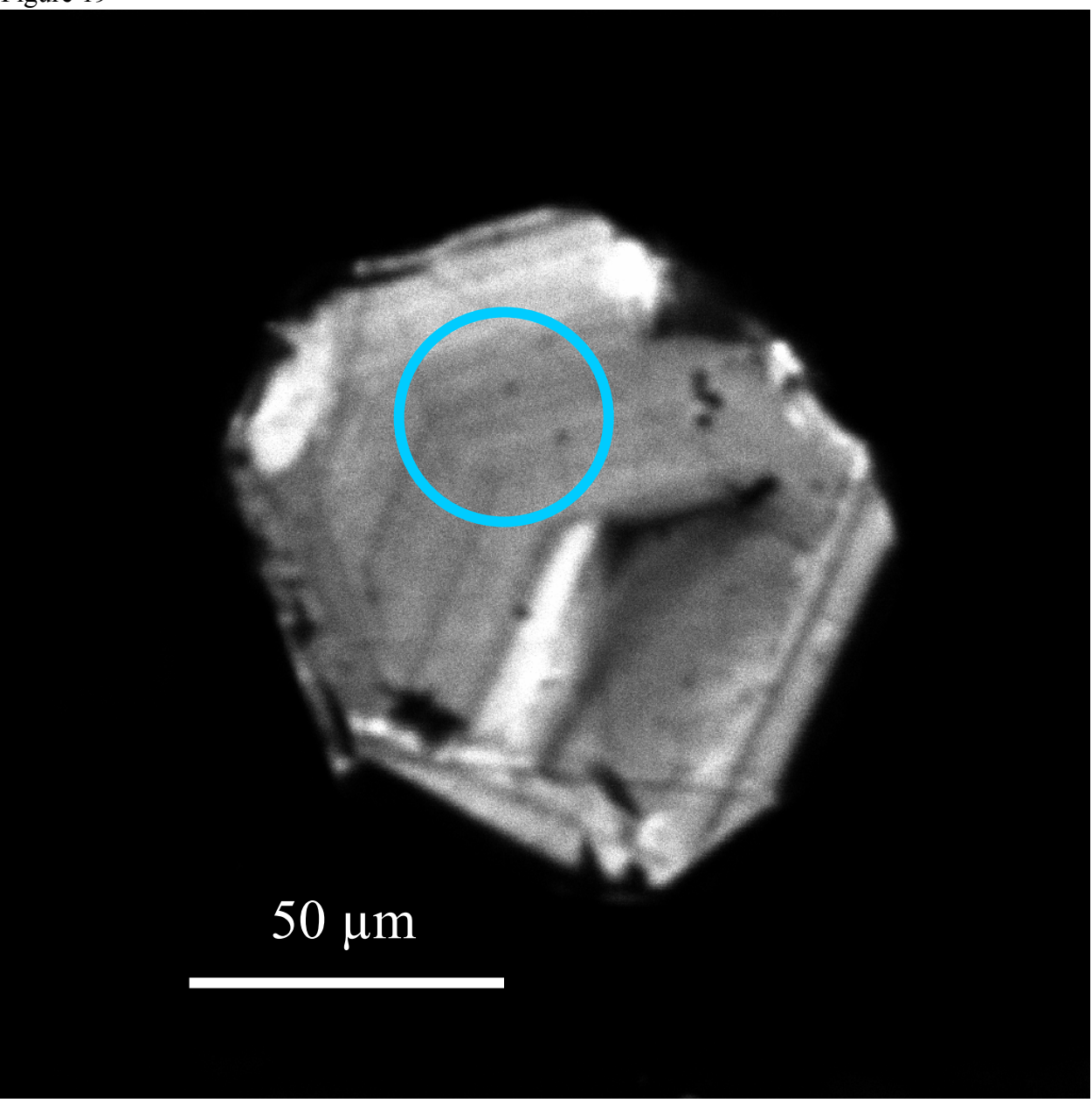
Concordance plot of zircon analyses from BIG-VA. Discordant points included. (Raum, 2008)

Figure 18



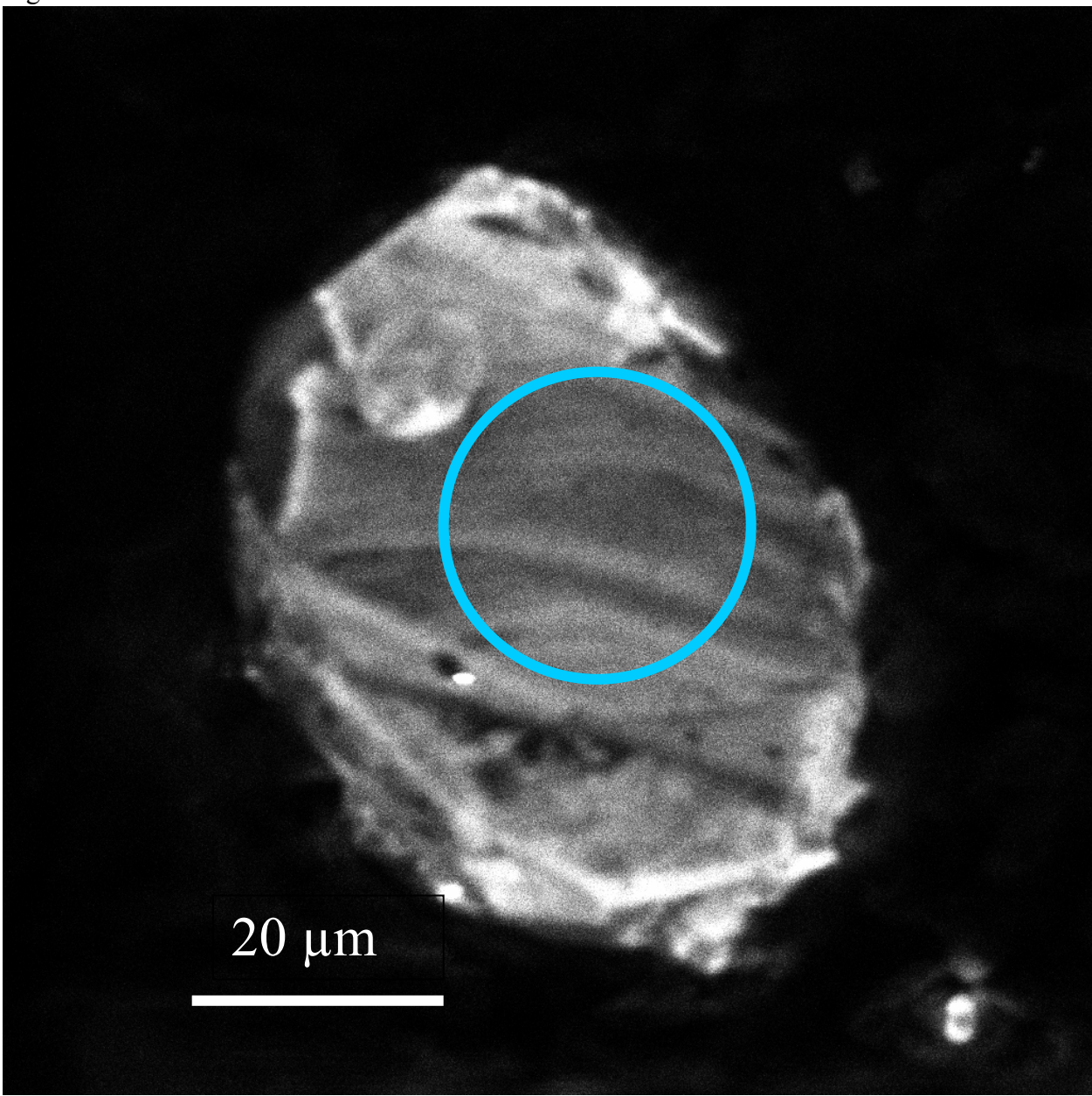
Concordance plot of zircon analyses from BIG-VA. Discordant points removed. (Raum, 2008)

Figure 19



Cathodoluminescence image of the youngest analyzed zircon from BIG-VA, showing the approximate size and placement of the laser spot. The calculated age is 571.1 Ma  $\pm$  37.4 (2 $\sigma$ ). (Raum, 2008)

Figure 20



Cathodoluminescence image of the oldest analyzed zircon from BIG-VA, showing the approximate size and placement of the laser spot. The calculated age is 1557.8 Ma  $\pm$  77.1 (2 $\sigma$ ). (Raum, 2008)

Table 1

BIG-VA	BIG-MD
N: 38° 58.623'	N: 38° 58.992'
W: 077° 14.446'	W: 077° 13.822'
Strike: 190°	Strike: 052°
Dip: 38° SE ~ granodiorite orientation	Dip: 46° NW ~ metasedimentary fold
Strike: 165°	Strike: 183°
Dip: 85° NE ~ schist foliation	Dip: 62° SE ~ metasedimentary fold

Summary of measurements taken at both Virginia and Maryland outcrops locations.

Table 2

Laser Parameters	BIG-VA	BIG-MD
Repetition rate	10 Hz	10 Hz
Power	54%	54%
Energy density	$2.23 \text{ J/cm}^2$	$2.23 \text{ J/cm}^2$
Spot diameters	30 μm, 40 μm	15 μm, 30 μm

Laser parameters used for LA-ICP-MS analytical sessions for BIG-VA and BIG-MD.

Table 3							
Sample name	<sup>207</sup> Pb/ <sup>235</sup> U	2 sigma	<sup>206</sup> Pb/ <sup>238</sup> U	2 sigma	RHO	<sup>207</sup> Pb/ <sup>206</sup> Pb	2 sigma
namo	intercept	abs err	intercept	abs err	11110	average	abs err
Ap04a146	2.777307	0.226850	0.235415	0.015952	0.842	0.085537	0.003775
Ap04a144	3.390712	0.300691	0.176168	0.012088	0.723	0.139551	0.008566
Ap04a142	4.948203	0.469811	0.208926	0.014276	0.609	0.171720	0.013051
Ap04a140	2.704051	0.235283	0.223827	0.016315	0.837	0.087593	0.004165
Ap04a138	1.911153	0.155404	0.138612	0.009369	0.846	0.099968	0.004341
Ap04a136	1.978341	0.159679	0.180807	0.012196	0.855	0.079333	0.003321
Ap04a134	3.567591	0.300615	0.248427	0.017454	0.840	0.104122	0.004766
Ap04a124	3.119312	0.269004	0.239912	0.016888	0.804	0.094270	0.004837
Ap04a122	2.136315	0.173476	0.193957	0.013170	0.854	0.079859	0.003373
Ap04a120	2.106833	0.172205	0.196017	0.013326	0.845	0.077930	0.003408
Ap04a118	2.427075	0.197544	0.215997	0.014614	0.845	0.081471	0.003543
Ap04a116	2.450325	0.200111	0.220140	0.014943	0.844	0.080703	0.003533
Ap04a114	2.061989	0.171900	0.189419	0.013005	0.826	0.078927	0.003713
Ap04a100	2.020622	0.170123	0.187846	0.013212	0.842	0.077992	0.003538
Ap04a98	3.416499	0.296189	0.245284	0.017109	0.783	0.100990	0.005454
Ap04a96	3.085894	0.260991	0.194152	0.013187	0.787	0.115241	0.006015
Ap04a94	2.215165	0.184147	0.199008	0.013660	0.830	0.080705	0.003742
Ap04a92	3.102275	0.252023	0.240283	0.016292	0.851	0.093610	0.003990
Ap04a90	3.044213	0.246593	0.237202	0.016084	0.856	0.093052	0.003894
Ap04a80	1.936931	0.158362	0.184520	0.012565	0.847	0.076109	0.003311
Ap04a78	2.786613	0.231645	0.177254	0.011919	0.802	0.113985	0.005662
Ap04a76	3.309208	0.270776	0.264649	0.018150	0.855	0.090661	0.003847
Ap04a74	2.907527	0.235977	0.225729	0.015380	0.860	0.093390	0.003873
Ap04a72	2.501654	0.216559	0.176037	0.012034	0.758	0.103036	0.005829
Ap04a70	1.639104	0.134257	0.151090	0.010336	0.850	0.078657	0.003395
Ap04a58	1.059910	0.091018	0.122007	0.008612	0.815	0.062987	0.003137
Ap04a56	1.047605	0.090393	0.120341	0.008552	0.816	0.063117	0.003148
Ap04a54	2.337810	0.207848	0.194437	0.014694	0.853	0.087176	0.004050
Ap04a52	2.606727	0.222285	0.219822	0.015909	0.861	0.085979	0.003729
Ap04a50	3.849278	0.322552	0.241890	0.016964	0.846	0.115379	0.005150
Ap04a48	2.387091	0.199703	0.214184	0.014810	0.829	0.080807	0.003776
Ap04a26	3.487514	0.282023	0.261997	0.017745	0.858	0.096513	0.004015
Ap04a24	2.076452	0.171415	0.163813	0.011204	0.837	0.091905	0.004157
Ap04a22	2.083932	0.172271	0.194154	0.013312	0.838	0.077822	0.003514
Ap04a20	0.782396	0.065808	0.092636	0.006353	0.809	0.061237	0.003026
Ap04a18	2.930063	0.238851	0.240573	0.016410	0.854	0.088307	0.003747
Ap04a16	2.348562	0.191122	0.208304	0.014117	0.848	0.081747	0.003528
Ap04a14	2.249090	0.181348	0.202647	0.013657	0.856	0.080470	0.003360
Ap04a12	2.401663	0.196037	0.214068	0.014530	0.845	0.081344	0.003552
Summary of isotopic ratios from analysis of BIG-VA zircons.							

Table 4							
Sample name	<sup>207</sup> Pb/ <sup>235</sup> U	2 sigma	<sup>206</sup> Pb/ <sup>238</sup> U	2 sigma	<sup>207</sup> Pb/ <sup>206</sup> Pb	2 sigma	
	age	abs err	age	abs err	age	abs err	
Ap04a146	1349.5	60.1	1362.8	83.0	1327.7	84.2	
Ap04a144	1502.3	68.4	1046.0	66.1	2221.6	104.5	
Ap04a142	1810.5	78.7	1223.1	75.9	2574.5	124.3	
Ap04a140	1329.6	63.5	1302.1	85.7	1373.6	90.1	
Ap04a138	1085.0	53.5	836.8	52.9	1623.5	79.7	
Ap04a136	1108.2	53.7	1071.4	66.4	1180.4	81.7	
Ap04a134	1542.4	65.8	1430.4	89.8	1698.9	83.2	
Ap04a124	1437.5	65.2	1386.2	87.5	1513.5	95.3	
Ap04a122	1160.6	55.4	1142.8	70.9	1193.5	82.2	
Ap04a120	1151.0	55.5	1153.9	71.6	1145.1	85.7	
Ap04a118	1250.7	57.7	1260.7	77.2	1232.8	84.2	
Ap04a116	1257.5	58.1	1282.6	78.7	1214.2	84.9	
Ap04a114	1136.3	56.2	1118.2	70.3	1170.3	91.8	
Ap04a100	1122.5	56.4	1109.7	71.5	1146.7	88.8	
Ap04a98	1508.2	67.0	1414.1	88.3	1642.4	98.6	
Ap04a96	1429.2	63.8	1143.8	71.0	1883.7	92.5	
Ap04a94	1185.8	57.3	1170.0	73.2	1214.3	89.9	
Ap04a92	1433.3	61.4	1388.2	84.4	1500.3	79.5	
Ap04a90	1418.8	61.0	1372.1	83.5	1488.9	78.2	
Ap04a80	1093.9	54.0	1091.6	68.2	1097.9	85.9	
Ap04a78	1352.0	61.2	1052.0	65.1	1863.9	88.3	
Ap04a76	1483.2	62.8	1513.6	92.2	1439.5	79.8	
Ap04a74	1383.9	60.4	1312.1	80.6	1495.8	77.5	
Ap04a72	1272.5	61.8	1045.3	65.8	1679.5	102.7	
Ap04a70	985.4	51.0	907.1	57.8	1163.5	84.4	
Ap04a58	733.8	44.4	742.1	49.4	707.8	104.2	
Ap04a56	727.7	44.3	732.5	49.1	712.2	104.3	
Ap04a54	1223.9	62.3	1145.4	79.1	1364.4	88.2	
Ap04a52	1302.5	61.6	1280.9	83.8	1337.7	82.7	
Ap04a50	1603.1	66.4	1396.5	87.8	1885.8	79.3	
Ap04a48	1238.7	59.0	1251.1	78.4	1216.8	90.6	
Ap04a26	1524.4	62.8	1500.1	90.3	1557.8	77.1	
Ap04a24	1141.1	55.8	977.9	61.9	1465.4	84.7	
Ap04a22	1143.5	55.9	1143.8	71.7	1142.3	88.5	
Ap04a20	586.8	37.1	571.1	37.4	647.6	104.4	
Ap04a18	1389.7	60.8	1389.7	85.0	1389.2	80.4	
Ap04a16	1227.1	57.1	1219.8	75.1	1239.5	83.4	
Ap04a14	1196.5	55.9	1189.5	73.0	1208.5	81.1	
Ap04a12	1243.1	57.7	1250.5	76.9	1229.8	84.5	
Summary of ages from analysis of BIG-VA zircons.							

# APPENDIX

I pledge on my honor that I have not given or received any unauthorized assistance on this assignment.